π-electron delocalization in poly(*p*-phenylene), poly(*p*-phenylene sulfide), and poly(*p*-phenylene oxide)

G. Crecelius
Institut für Festkörperforschung, Kernforschungsanlage Jülich, Postfach 1913, D-5170 Jülich, Germany

J. Fink
Kernforschungszentrum Karlsruhe GmbH, Institut für Angewandte Kernphysik I, Postfach 3640, D-7500 Karlsruhe, Germany

J. J. Ritsko
Institut für Festkörperforschung, Kernforschungsanlage Jülich, Postfach 1913, D-5170 Jülich, Germany and Xerox Webster Research Center, Xerox Square-114, Rochester, New York 14644

M. Stamm
Institut für Festkörperforschung, Kernforschungsanlage Jülich, Postfach 1913, D-5170 Jülich, Germany

H.-J. Freund and H. Gonska
Lehrstuhl für Theoretische Chemie, Universität Köln, Greinstrasse 4, D-5000 Köln 41, Germany
(Received 28 February 1983)

As deduced from electron-energy-loss experiments, the π band in poly(*p*-phenylene) has a width comparable to that in graphite. The π-band width in poly(*p*-phenylene sulfide) is considerably narrower, and in poly(*p*-phenylene oxide) the π electrons are localized in benzene-derived states. These results are in line with recent theoretical results. In addition, structure in the C $1s$–π^* absorption is shown to be due to chemical shifts of C atoms in different coordination.

INTRODUCTION

It has recently been reported[1] that poly(*p*-phenylene) (PPP) has been synthesized in both the undoped and AsF_5-doped form. Pristine PPP is a relatively good insulator with a conductivity of the order of $10^{-10}\ \Omega^{-1}\,cm^{-1}$. Since low-molecular-weight oligomers of PPP up to sexiphenyl are known to exist, a fundamental question in PPP is to what degree the π electrons are delocalized. Gillam and Hey[2] have measured optical abosorption in systems up to sexiphenyl and observe an energy shift of the absorption maximum from 6.17 eV in benzene to 3.9 eV in sexiphenyl, which they take as an indication of appreciable delocalization of the π electrons. As their samples were solutions of polyphenyls in different solvents, no conclusions on any degree of intermolecular delocalization can be drawn from their results.

Quite recently, Riga *et al.*[3] have reported on an x-ray photoelectron spectroscopy (XPS) study of both the valence band and the C $1s$ core state of the series up to *p*-quaterphenyl and PPP. Comparison with similar data for the lower acenes and polystyrene leads them to conclude that π-electron delocalization in the *p*-polyphenyls is weak and essentially intramolecular as indicated by a broadening and energy lowering of the highest occupied π levels.

The band structure of a PPP chain has been calculated by Whangbo *et al.*,[4] Grant and Batra,[5] and Brédas *et al.*[6] The width of the highest occupied π band according to their results is about 3 eV, which is taken as an indication of large π overlap and delocalization. In addition, a quite flat π band is predicted at somewhat higher binding energy. Riga *et al.*[3] have stated that the result of Grant and Batra[5] is not necessarily contradictory to their experimental finding as they define delocalization in the polyphenyls with respect to acenes and polystyrene. On the other hand, XPS experiments in this case give no reliable estimate of the full width of the highest occupied π band. More direct information on the relative width of the π bands is obtained from a study of the dynamical properties of the π-band electrons. Electron-energy-loss spectroscopy (EELS) offers a unique possibility to study such effects by measuring the wave-vector dependence of π-electron excitations provided these excitations are sufficiently delocalized. In the free-electron model, those excitations are referred to as plasmons.[7]

As has already been suggested by Riga *et al.*,[3] we have undertaken as EELS study of PPP, poly(*p*-phenylene sulfide) (PPS), and poly(*p*-phenylene oxide) (PPO), both pure and with methyl side groups (see Fig. 4). By inserting heteroatoms S and O between the phenyl groups, the degree of delocalization of the π electrons is supposed to be reduced. We have studied excitations in the three systems both in the energy range of the valence excitations and the C $1s$ excitation. From the valence excitations the fundamental electronic transitions are obtained by means of a Kramers-Kronig analysis. From the wave-vector dependence of the energy of these excitations their spatial extent is deduced. The magnitude of the dispersion constant is a direct measure of the degree of delocalization of the electrons participating in the excitation.

In PPP we observe an excitation which, with respect to its dispersive behavior, closely resembles the π plasmon in

graphite.[8] An additional spectroscopic feature is identified due to π-π^* transitions which are confined to the weakly distorted benzene ring. The width of this peak supplies information on the strength of the interaction between the benzene rings which is also a measure of the degree of π-electron delocalization. The portion of the C 1s excitation to π-derived final states, which we call s-π^* for brevity, contains some structure which shows the distinction between carbon atoms in different coordination.

EXPERIMENTAL

EELS was carried out using a newly designed spectrometer with a primary energy $E_0 = 170$ keV. The energy resolution was $\Delta E = 0.1$ eV and the momentum resolution $\Delta q = 0.03$ Å^{-1} at a beam current of about 1 nA. The scattering chamber of the spectrometer was part of an ultrahigh-vacuum (UHV) system which allowed heat treatment of the samples in a vacuum less than 10^{-7} Pa and transfer into the electron beam without breaking the vacuum. EELS requires thin-film samples with an area of about 0.25 mm^2 and a thickness of the order of the primary electron mean free path which in our case was about 1000 Å.

Both PPS and PPO are available commercially from Aldrich and Polysciences, respectively, and thin films are obtained by producing dilute solutions which are dispersed on either NaCl or glass substrates for PPS and PPO, respectively, and floated off in distilled water or alcohol after evaporating the solvent. The starting material for our PPO samples contained reasonable amounts of polystyrene. To check the influence of the polystyrene content on our spectra of the PPO sample, a valence-excitation spectrum of pure polystyrene has also been recorded and plotted as the broken curve in Fig. 1. The C 1s excitation spectrum of polystyrene is exhibited as the dotted curve in Fig. 4. Especially the latter one ensures that there seems to be only a minor contribution of the polystyrene content to our PPO results. PPP is insoluble and has to be prepared by polymerizing benzene with a suitable catalyst. Samples were prepared by the Kovacic or the Yamamoto method[9] at room temperature using benzene, $CuCl_2$, and $AlCl_3$ or dibromobenzene, $CoCl_2$, Mg, and tetrahydrofuran, respectively. The reaction product was washed with HCl and distilled water.

The most severe problem was imposed by the necessity to produce thin continuous films. In most cases the best approach was a two-dimensional agglomerate of extremely fine powder which was obtained by introducing a microscope mesh into a suspension of the PPP powder in distilled water.

The crystallinity of the samples was checked by recording diffraction patterns with the EELS spectrometer at zero energy loss and variable momentum transfer. In all cases the as-grown material displayed an electron-diffraction pattern consisting of an amorphous halo. PPP samples were heat treated at 420 °C for 24 h, both PPS and PPO samples at 240 °C for 2 h, and afterwards the diffraction pattern displayed good crystallinity except for both PPO species. The degree of crystallinity had, however, only a minor influence on the shape of the structures in the energy-loss spectrum.

The spectra were subject to much more distortion after prolonged exposure to beam currents in excess of 1 nA because of radiation damage. The diffraction pattern of a severely radiation-damaged sample also showed an amorphous halo but in this case the structure of the valence-excitation spectrum was both shifted and broadened. As is expected from thermal stability, PPP is more resistant against radiation damage than both PPS and PPO.

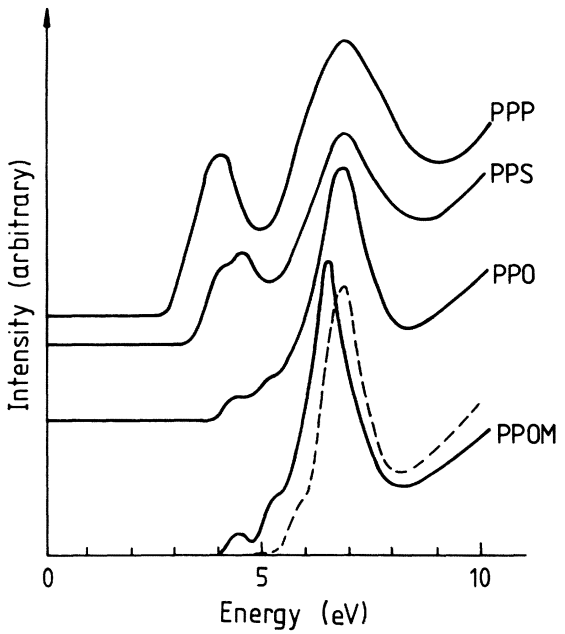

FIG. 1. Energy-loss spectra of the valence-excitation regime of PPP, PPS, PPO, and PPOM. Broken curve is for polystyrene.

RESULTS

Typical loss spectra for the regime of the valence-excitations of PPP, PPS, PPO, and poly(3,5-dimethylphen-1,4-ylene oxide) (PPOM) are shown in Fig. 1 for a momentum transfer of 0.08 Å^{-1}. The most pronounced structure in these spectra is a peak at about 7 eV which is at slightly lower energy in the PPOM, but is considerably narrowed in proceeding from PPP to PPOM via PPS and PPO. This structure remains unaltered in energy with an increasing wave vector which is a clear indication that the electrons participating in this excitation are strongly localized. In PPP we observe an additional, slightly weaker excitation at about 4 eV. The energy of this transition increases with decreasing wavelength according to

$$\hbar\omega = \hbar\omega_0 + \alpha(\hbar^2/m)q^2 \ , \tag{1}$$

with $\alpha = 1.15$. Figure 2 shows the momentum dependence of the valence excitations in PPP. The momentum dependence of the energy of the 4-eV excitation is shown in the inset to be linear with q^2. The intensity decreases quite rapidly with respect to the 7-eV excitation upon increasing wave vector. All features characterizing this excitation are strongly reminiscent of the description of a plasmon, hence a strongly delocalized excitation. In PPS the 4-eV structure is shifted to slightly higher energy and split into

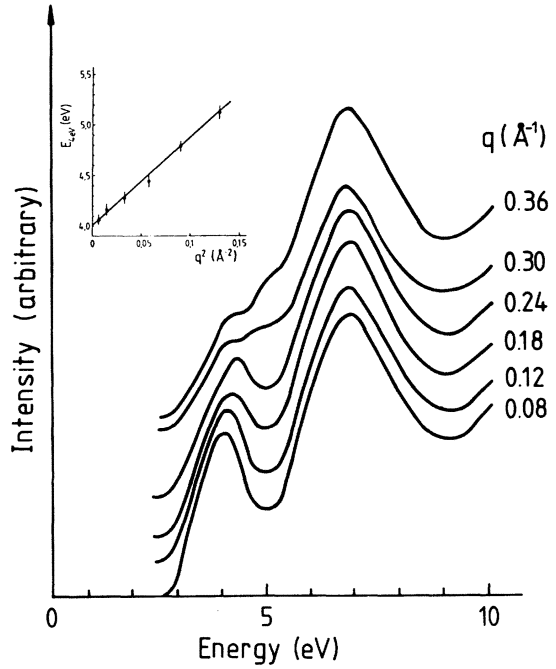

FIG. 2. Energy-loss spectra of the valence-excitation regime of PPP as a function of momentum transfer q. The peak at 4 eV reappearing at the two highest momenta is due to a double scattering process, one elastic with $q=q_0$ and one inelastic with $E=4$ eV and $q=0$. The momentum dependence of the energy of the 4-eV loss is shown in the inset to be linear with q^2.

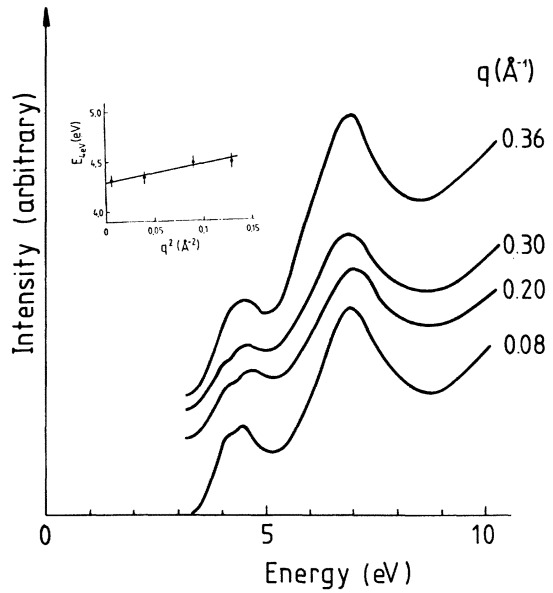

FIG. 3. Energy-loss spectra of the valence-excitation regime of PPS as a function of momentum transfer q. Inset shows the momentum dependence of the energy of the 4-eV loss to be linear with q^2, although α is much smaller than in PPP.

two peaks with different intensities. According to Giovanelli *et al.*[10] there should be low-lying transitions between free-electron pairs of the heteroatom and the π^* orbitals of the phenyl groups. These may be responsible for the splitting of 4-eV loss in PPS. The intensity relative to the 7-eV structure in this case also decreases quite rapidly with increasing momentum transfer. The energy, however, increases only slightly with increasing wave vector as is shown in Fig. 3. A reasonable fit is obtained using a q^2 dependence according to Eq. (1) with $\alpha=0.2$, as demonstrated by the inset in Fig. 3. As a result, in PPS we also observe an excitation at about 4 eV which displays properties typical for transitions between delocalized electron states.

Both PPO and PPOM show weak structure at about 4.5 eV and a shoulder at about 5.4 eV which is independent of wave vector with respect to both energy and intensity. Hence both features are associated with well-localized transitions. In summary, from our energy-loss data in the region of the valence excitations we conclude that in all four systems we have a strong transition between well-localized states at about 7 eV. In addition, both PPP and PPS display excitations at about 4 eV which are characterized by properties typical for transitions between delocalized states which are reminiscent of plasmons in the free-electron model.

As is clearly visible in Fig. 1, all four systems show a sharp onset of absorption above a well-defined gap the width of which is 2.85 eV for PPP, 3.4 eV in PPS, and 4 eV in both PPO species. Our band gap of 2.85 eV is slightly narrower than the theoretical result of 3.5 eV obtained by Brédas *et al.*[6] from band-structure calculations. The gap width is independent of the wave vector in our samples.

The spectra obtained in the region of the C $1s$—π^* transition in all four materials are shown in Fig. 4. It is espe-

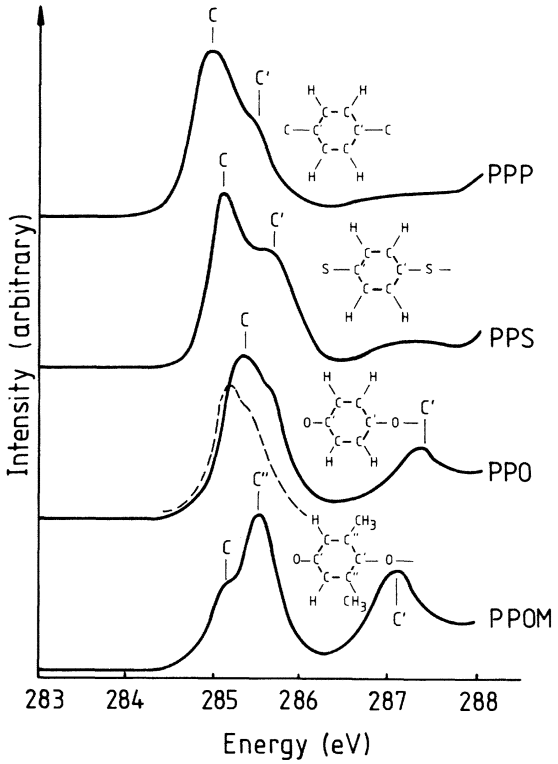

FIG. 4. Energy-loss spectra of the C $1s$—π^* excitation regime of PPP, PPS, PPO, and PPOM. The correspondence between loss features and carbon species is indicated. Broken curve is for polystyrene.

cially noteworthy that the edge is shifted from 284.4 eV in PPP to 284.7 eV in PPS and to 284.8 eV in both PPO species. In addition, we observe structures shifted towards higher energy by about 0.5 eV.

DISCUSSION

To understand our data and to possibly obtain some insight into the question raised at the beginning of this paper as to what degree the π states in polyphenylene and its derivatives are delocalized, it is useful to discuss our results in the context of what is already known about extended π-electron systems. The prototype of these systems is graphite. Results of experiments have been reviewed by Daniels *et al.*[8] A polymer which has become a classic in this respect is polyacetylene (PA), detailed EELS investigations on which have been reported by Ritsko *et al.*[11]

To discuss our results in this framework, we start with the spectrum of valence excitations in PPP up to an energy of 40 eV. Shown in Fig. 5(a) is the energy-loss function $\mathrm{Im}(-1/\epsilon)$ of PPP at a momentum transfer of 0.1 Å^{-1}, which has been deduced from the energy-loss spectrum by correcting for finite momentum resolution and multiple energy losses. The loss function is dominated by a broad structure at about 25 eV which closely resembles the loss function in both graphite and PA. At lower energy, Fig. 5(a) shows the weak structures at 4 and 7 eV already mentioned in Fig. 1. This is at variance with graphite and PA because in both these cases only one structure is observed in this energy range. (The energy of this excitation is at 7 eV in graphite[8] and at 4 eV in PA,[11] but this coincidence with the energy position of the structures in PPP is accidental and of no importance.)

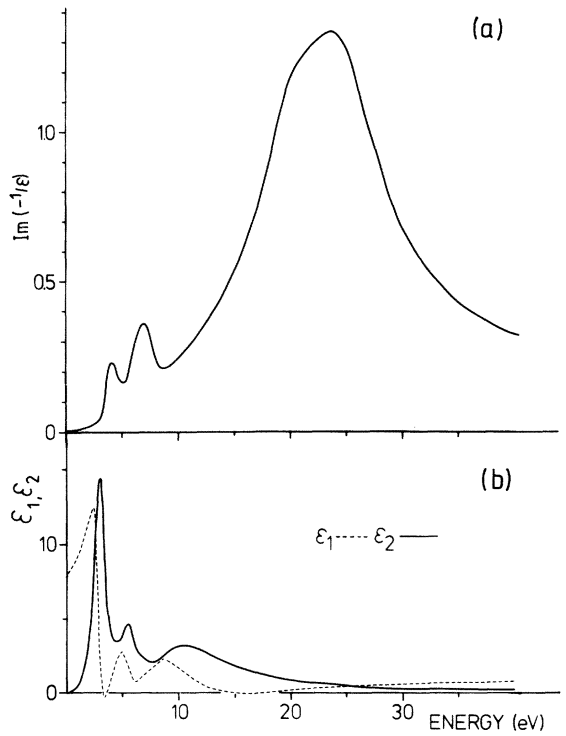

FIG. 5. (a) Energy-loss function of PPP as deduced from energy-loss spectrum. (b) Real and imaginary part of the dielectric function of PPP as obtained by Kramers-Kronig analysis from the loss function. For details, see text.

The fundamental electronic excitations responsible for the shape of the energy-loss function are obtained by a Kramers-Kronig analysis, the results of which are shown in Fig. 5(b). There are two strong interband transitions in PPP contributing to the imaginary part of the dielectric function: one at 2.9 eV and one at 10.4 eV. In graphite there are also two interband transitions contributing to ϵ_2 at 4.5 and at 14.5 eV, which in this case correspond to transitions between π-π^* and σ-σ^* states, respectively, and in PA the situation is the same with somewhat different energy separations. Both these interband transitions drive the real part of ϵ to very small values. (In Fig. 5, ϵ_1 is even driven negative in both cases, but as ϵ_1 has to be adjusted at zero energy to the static dielectric constant, which is not known, the exact value of ϵ_1 at the minima is somewhat arbitrary.) Zeros in ϵ_1 lead to maxima in the energy-loss function.

All three band-structure calculations[4-6] predict a wide π band as the highest occupied one which is derived from $2p_z$ orbitals on carbon atoms connecting the phenyl groups. At slightly higher binding energy they find a quite flat π band, which is flat because it has almost no contribution from $2p_z$ wave functions, because there are nodes on the C atoms connecting the rings. At even higher binding energy there are further π and σ bands that are rather wide. Transitions between the wide π and σ bands and the corresponding unoccupied π^* and σ^* bands are identified with the strong interband transitions at 2.9 and 10.4 eV in Fig. 5. Hence both these π-π^* and σ-σ^* transitions involve delocalized electrons and correspond to collective excitations in the free-electron model which are called plasmons. For brevity, we henceforth call the energy-loss features at 4 and 25 eV in the loss function π and $\pi+\sigma$ plasmon in analogy with graphite and PA.

As has been mentioned, the 4-eV structure, which we call π plasmon, disperses quadratically with a dispersion constant $\alpha=1.15$; see the inset in Fig. 2. This behavior is in line with that of a plasmon in a free-electron band. In the random-phase approximation (RPA), α is given by[12]

$$\alpha_{\mathrm{RPA}}=\frac{3}{5}\frac{E_F}{\hbar\omega_{P_0}} ,$$

where E_F is the Fermi energy and ω_{P_0} is the plasma frequency at $q=0$.

Scaling the π-plasmon dispersion constant of graphite $\alpha_{\mathrm{gr}}=0.58$ with the ratio of the $q=0$ plasmon energies of graphite and PPP leads to

$$\tilde{\alpha}_{\mathrm{gr}}=1.1$$

(where $\tilde{\alpha}$ denotes scaling) which is close to the value of α_{PPP} as deduced from our results.

Arguing in the framework of the free-electron model, this means that the width of the π band in PPP is comparable with that in graphite and the same is true for the degree of delocalization of the π electrons. The width of the highest occupied π band in graphite is found to be about 7.5 eV in the band-structure calculation of Painter and

Ellis, and this value is in agreement with some more recent calculations.[13] A very recent band-structure calculation of PPP by Brédas *et al.*[6] yields 3.5 eV for the width of the highest occupied π band in PPP in agreement with Grant and Batra's result.[5] Both these theoretical results confirm our experimental estimate. The reduction in π-plasma frequency from the graphite value of 7 to 4 eV is mainly due to a reduced electron concentration.

In addition to interband transitions at 2.9 and 10.4 eV shown in Fig. 5, there is another one at 5.4 eV in PPP which is missing in both graphite and PA. It gives rise to the energy-loss peak at about 7 eV shown in Figs. 1 and 5. Although no clear distinction as to the nature of this transition is possible from the behavior of the dielectric function, the independence of wavelength as demonstrated in Fig. 2 strongly suggests that this excitation is a localized transition. This characterization of the loss leads us to identify it with transitions between the flat π and π^* bands described above.

To further elucidate the nature of this energy loss we have taken valence-excitation spectra (Fig. 6) in polystyrene and polycarbonate (PC), both of which contain benzene rings either singly connected as in polystyrene or in a para-double connection as in PPP or PC. In polyvinylcarbazole the benzene ring has only two double bonds left. In all systems where the benzene ring is coordinated as in PPP or PC, we find a narrow dispersionless excitation at 7 eV. In polyvinylcarbazole, however, where there are only two double bonds left in the benzene ring, there are two such excitations at 5.8 and 7.7 eV which also show no dispersion, as shown in Fig. 6.

From this we conclude that the 7-eV excitation in PPP, PPS, and PPO is a transition which is confined to the benzene ring. It is reminiscent of the most prominent $^1A_{1g} \rightarrow {}^1E_{1u}$ transition in benzene.[14] With this assignment we are also able to identify the two weak structures in the valence-excitation spectra of PPO and PPOM at 4.5 and 5.4 eV, shown in Fig. 1. These transitions are almost identical to those of benzene.[15] As has already been pointed out by Ritsko[16] in the context of EELS investigations of polystyrene, the 4.75-eV transition is symmetry forbidden in benzene. In PPO and PPOM, as well as in polystyrene and polycarbonate, the benzene-ring symmetry is sufficiently distorted to make this transition slightly allowed (and to eventually cause some energy shift), see Fig. 6.

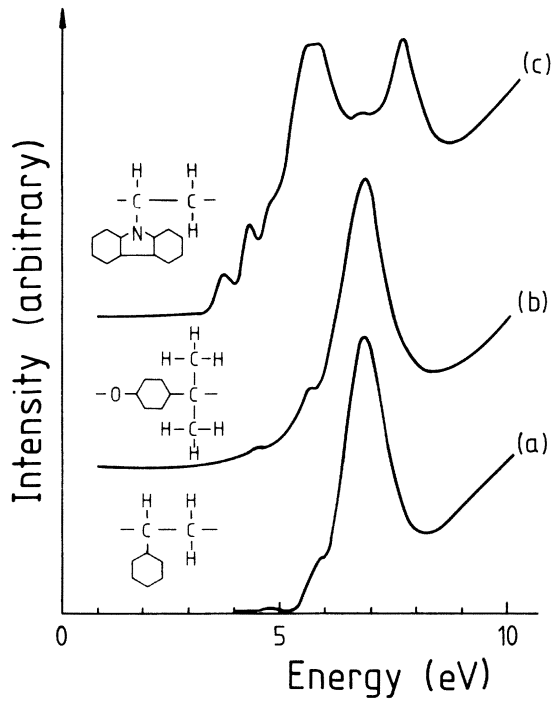

FIG. 6. Energy-loss spectra of the valence-excitation regime of polystyrene (a), polycarbonate (b), and polyvinylcarbazole (c). Formulas indicate only coordination of phenyl groups.

Further evidence for this nature of the 7-eV energy-loss structure comes from the XPS investigation of the polyphenyls of Riga *et al.*[3] They observe a strong satellite in the C 1*s* core-level spectra displaced 6.3 eV from the main peak, which they identify with a shake-up satellite. If we realize that the final state of a shake-up satellite observed in XPS is correlated with the final state of the π-π^* transition in optical absorption, as has been shown for benzene recently,[17] the existence of this shake-up satellite confirms our interpretation of the nature of the 7-eV loss.

To summarize the information we have obtained from Fig. 5 about the valence excitation in PPP: The 4-eV structure is due to a collective excitation which is to be regarded in analogy with a π plasmon in a nearly-free-electron band. The structure at about 7 eV is due to a π-π^* transition which proceeds between well-localized states confined to individual benzene rings.

The dielectric function of PPS is qualitatively in line with that of PPP, Fig. 5. There are also three interband transitions contributing to ϵ_2 at about 3, 5, and 8.5 eV. The latter can readily be associated with a $\pi+\sigma$ plasmon at about 22 eV in the loss function as in PPP. The 5-eV transition has the same origin as in PPP, Fig. 5, giving rise to the localized 7-eV transition in the loss function ascribed to benzene states.

As has been mentioned, the loss peak corresponding to the 3-eV interband transition in PPS displays properties of a transition between delocalized states, but to a much lesser extent than the corresponding transition in PPP. In fact, the dispersion constant $\alpha_{\mathrm{PPS}}=0.2$, as shown in the inset in Fig. 3, if scaled with the ratio of the $q=0$ plasmon energies of PPS and graphite to correct for the smaller PPS plasma frequency, gives $\tilde{\alpha}_{\mathrm{PPS}}=0.12$ as compared to $\alpha_{\mathrm{gr}}=0.58$. From this we conclude that the π-band width and hence the delocalization of the π electrons in PPS is considerably smaller than in PPP. Brédas's band-structure calculations[6] give a width of the highest occupied π band in PPS of 1.2 eV, which is roughly a factor of 3 less than in PPP. Hence we conclude that the 4-eV loss structure in PPS is due to transitions between delocalized states, but the width of the associated band is much smaller than in PPP. If we use the plasmon picture, we would have to refer to a plasmon in a narrow tight-binding band.

In both PPO species all plasmonlike losses except the $\pi+\sigma$ plasmon at about 22 eV are absent. As we have pointed out, all losses below 10 eV must be ascribed to localized transitions between states in the benzene ring. We conclude that the π electrons in PPO are completely localized in the phenyl groups. This view is further supported by the reduction of the linewidth of the 7-eV peak in Fig. 1 from PPP to PPO. Our results concerning the width of

the π band in PPP, PPS, and PPO are at variance with results of band-structure calculations of Duke and Paton.[18] They predict that in all three compounds the lowest binding energy molecular-ion states are π-electron states which extend throughout the molecule.

In Fig. 4 we show the loss spectra in the regime of the carbon k shell excited to π-derived final states. The spectra do not reflect the density of unoccupied states.[19] They are interpreted by an interaction of the conduction band with the core hole leading to strong resonancelike absorption at the bottom of the conduction band. The structure in the loss spectrum in the energy region of C $1s$—π^* transition in PPP [upper curve in Fig. 4(a)] is readily understood qualitatively by realizing that, if we restrict our considerations to nearest neighbors in two dimensions, carbon atom C′ is identical to a carbon atom in graphite, whereas atom C is identical to a carbon atom in *cis*-polyacetylene, see Fig. 4. In graphite the peak in the $1s$-π^* transition is at 285.3 eV (Ref. 20) and the corresponding structure in *trans*-PA is at 284.1 eV.[21] From this we tentatively associate the loss peak at higher transition energy in the PPP spectrum of Fig. 4 with absorption in the carbon atom C′ and the lower-energy peak with atoms C. Confidence with this assignment comes from regarding electronegativities. By using the Allred-Rochow formula,[22] the electronegativity of hydrogen is about 10% smaller than that of carbon. Hence the hydrogen-substituted carbon atoms carry a larger electron density than the carbon atoms C′ connecting the benzene rings, resulting in a smaller binding energy of the C $1s$ level and a smaller C $1s$—π^* transition energy. Further support for this assignment is furnished by explicit molecular orbital (MO) calculations of the complete neglect of differential overlap (CNDO) type[23] on a series of model molecules,[24] namely oligo-*p*-phenylenes as shown in Fig. 7. The result borne out by these calculations is the same as the one reached by electronegativity considerations: The larger electronegativity of carbon relative to hydrogen leads to a decreased electron density of carbon atoms C′. As is shown by the calculations, the difference in electron population of 0.07 electrons between the two carbon atoms is basically not affected by increasing the chain length.

With the use of this electronegativity-type argument it becomes immediately clear that the C $1s$-edge spectrum in PPS should be similar to that of PPP because carbon and sulfur electronegativities are about the same. Remembering the reduced π-electron delocalization in going from PPP to PPS and PPO, deduced from the valence excitations, and using the same shielding argument, we readily expect an increase in C $1s$-edge transition energy with decreasing π-electron delocalization. Both these conclusions are in line with the results in Fig. 4. Using MO theory, we have calculated the model compound shown in Fig. 7(a). Two benzene moieties linked by a sulfur atom are parasubstituted by thiomethoxy groups in order to terminate the chain. On the basis of the calculated electron density distributions, the $1s$—π^* transitions involving the peripheral carbon atoms C are expected at lower binding energies than those associated with carbon atoms C′. The density difference amounts to 0.04 electrons. This is the same order of magntiude as found for PPP. Relative to PPP, where the peripheral carbon atoms carry a slightly negative charge of -0.05 electrons, in PPS the corresponding carbon atoms are neutral. The shift of the loss edge, experimentally observed in PPS, is in line with these findings.

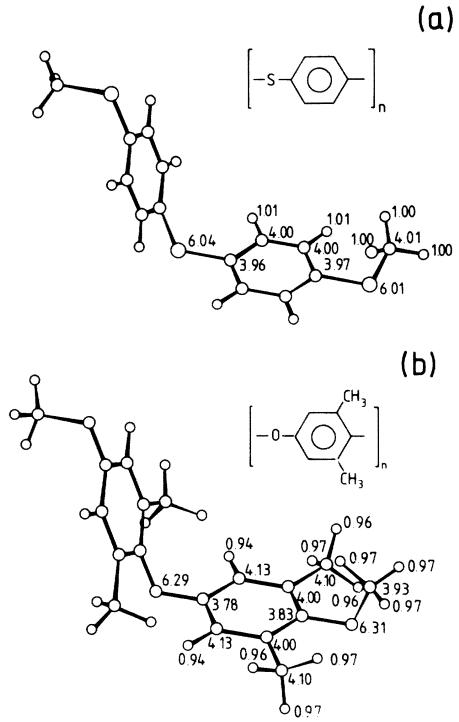

FIG. 7. Model molecules used in the CNDO-MO calculations of PPS and PPO (PPOM). The numbers give electron densities in number of electrons at the corresponding atom site.

In contrast with the sulfur electronegativity in PPS, the electronegativity of oxygen in PPO exceeds that of carbon by about 40%. This leads us to an assignment of spectral features in PPO to the two C atoms as given in Fig. 4. The assignment of loss peaks in PPOM as given in Fig. 4 is obtained from MO calculations on a model compound shown in Fig. 7(b). It is the oxygen analog of the sulphur compound, where two hydrogen atoms of each benzene moiety are substituted by methyl groups. As expected from the electronegativity arguments, the charge of the carbon atoms connnected to the oxygen is considerably larger than in PPP and PPS, namely, 0.22 electrons. The other carbon atoms in the system carry a similar charge as in PPS and PPP, respectively. In particular, carbon atom C'' is neutral and thus similar to the peripheral carbon atoms in PPS, while carbon atom C is negatively charged, similar to the carbon atoms in PPP. As the spectra shown in Fig. 4 only cover excitations to π-derived final states, no strong signal from the carbon atoms of the methyl groups is expected. Using the approximate relation between chemical shift and electron density $\Delta E = 6$ eV/e and the difference in electron count between C and C′, $\Delta e = 4.13 - 3.83e = 0.3e$ from Fig. 5(b), we estimate a chemical shift between signals C and C′ of about 1.8 eV, which is close to the separation of the corresponding peaks in Fig. 4.

In summary, we have presented evidence that the width of the highest occupied π band in PPP is comparable to

that in graphite. The corresponding band in PPS is much narrower, whereas the π electrons in PPO are localized in the phenyl group.

This follows from the existence of a plasmonlike excitation between states of varying degree of delocalization in PPP and PPS. In addition, we observe a localized excitation whose width depends on the width of the π band. In PPO no collective excitation is observed and the spectrum of valence excitations is explained by regarding excitations known from the benzene spectrum. Structure of the C $1s$—π^* excitation in the different compounds are explained by chemical shift of carbon atoms in different coordinations.

ACKNOWLEDGMENT

We are indebted to J. Pflüger for performing some of the Kramers-Kronig calculations. Experimental assistance by Frau B. Walker and F. P. Johnen is gratefully acknowledged.

[1]D. M. Ivory, G. G. Miller, J. M. Sowa, L. W. Shacklette, R. R. Chance, and R. H. Baughman, J. Chem. Phys. 71, 1506 (1979); L. W. Shacklette, H. Eckhardt, R. R. Chance, G. G. Miller, D. M. Ivory, and R. H. Baughman, *ibid.* 73, 4098 (1980); L. W. Shacklette, R. R. Chance, D. M. Ivory, G. G. Miller, and R. H. Baughman, Synth. Met. 1, 307 (1980).

[2]A. E. Gillam and P. H. Hey, J. Chem. Soc. (1939), 1170.

[3]J. Riga, J. J. Pireaux, J. P. Boutique, R. Caudano, and J. J. Verbist, Synth. Met. 4, 99 (1981).

[4]M. H. Whangbo, R. Hoffmann, and B. B. Woodward, Proc. R. Soc. London, Ser. A 366, 23 (1979).

[5]D. M. Grant and I. P. Batra, Synth. Met. 1, 193 (1980).

[6]J. L. Brédas, R. R. Chance, R. Silbey, G. Nicolas, and P. Durand, J. Chem. Phys. 77, 371 (1982).

[7]H. Raether, in *Solid State Excitations by Electrons Plasma Oscillations and Single Electron Transitions,* Vol. 38 of *Springer Tracts in Modern Physics,* edited by G. Höhler and E. A. Wiekisch (Springer, Berlin, 1965), p. 85.

[8]J. Daniels, C. Festenberg, H. Raether, and K. Zeppenfeld, in *Optical Constants of Solids by Electron Spectroscopy,* Vol. 54 of *Springer Tracts in Modern Physics,* edited by G. Höhler and E. A. Wiekisch (Springer, Berlin, 1970), p. 77.

[9]P. Kovacic and A. Kyriakis, J. Am. Chem. Soc. 85, 454 (1963); T. Yamamoto, Y. Hayashi, and A. Yamamoto, Bull. Chem. Soc. Jpn. 51, 2091 (1978).

[10]K. H. Giovanelli, J. Dehler, and G. Höhlneicher, Ber. Bunsenges. Phys. Chem. 75, 864 (1971).

[11]J. J. Ritsko, Mater. Sci. Res. 7, 337 (1981), and references therein.

[12]See, for example, K. Sturm, Adv. Phys. 31, 1 (1982).

[13]G. S. Painter and D. E. Ellis, Phys. Rev. B 1, 4747 (1970); J. Blinowski, Nguyen Hy Hau, C. Rigaux, J. P. Vieren, R. Le Toullex, G. Furdin, A. Hérold, and J. Melin, J. Phys. (Paris) 41, 47 (1980); L. Samuelson and I. P. Batra, J. Phys. C 13, 5105 (1980).

[14]E. E. Koch and A. Otto, Chem. Phys. Lett. 42, 476 (1972).

[15]R. W. Bigelow, J. Chem. Phys. 66, 4241 (1976).

[16]J. J. Ritsko, Jpn. J. Appl. Phys. 17, 231, Suppl. 17-2 (1978); J. J. Ritsko and R. W. Bigelow, J. Chem. Phys. 69, 4162 (1978).

[17]N. Kosugi and H. Kuroda, Chem. Phys. 61, 431 (1981); R. W. Bigelow and H.-J. Freund, J. Chem. Phys. 77, 5552 (1982).

[18]C. B. Duke and A. Paton, *Conductive Polymers* (Plenum, New York, 1981), p. 155.

[19]P.M.Th.M. van Attekum and G. K. Wertheim, Phys. Rev. Lett. 43, 1896 (1979).

[20]J. Fink, G. Crecelius, and R. Manzke (unpublished).

[21]J. J. Ritsko, Phys. Rev. Lett. 46, 849 (1981).

[22]A. L. Allred and E. G. Rochow, J. Inorg. Nucl. Chem. 5, 264 (1958).

[23]J. A. Pople and D. L. Beveridge, *Approximate Molecular Orbital Theory* (McGraw-Hill, New York, 1970); J. Del Bene and H. H. Jaffé, J. Chem. Phys. 48, 1807 (1968); 48, 4050 (1968); 49, 1221 (1968).

[24]To determine the geometry of model molecules, standard bond lengths and bond angles have been used.